Coherent Modulation of Quasiparticle Scattering Rates in a Photoexcited Charge-Density-Wave System

J. Maklar,[1] M. Schüler,[2] Y. W. Windsor,[1] C. W. Nicholson,[1, *] M. Puppin,[1, †] P. Walmsley,[2, 3] I. R. Fisher,[2, 3] M. Wolf,[1] R. Ernstorfer,[1, 4] M. A. Sentef,[5] and L. Rettig[1, ‡]

[1]*Fritz-Haber-Institut der Max-Planck-Gesellschaft, Faradayweg 4-6, 14195 Berlin, Germany*
[2]*Stanford Institute for Materials and Energy Sciences, SLAC National Accelerator Laboratory, 2575 Sand Hill Road, Menlo Park, CA 94025, USA*
[3]*Geballe Laboratory for Advanced Materials and Department of Applied Physics, Stanford University, Stanford, CA 94305, USA*
[4]*Institut für Optik und Atomare Physik, Technische Universität Berlin, Straße des 17. Juni 135, 10623 Berlin, Germany*
[5]*Max Planck Institute for the Structure and Dynamics of Matter, Luruper Chaussee 149, 22761 Hamburg, Germany*
(Dated: August 30, 2021)

We present a complementary experimental and theoretical investigation of relaxation dynamics in the charge-density-wave (CDW) system TbTe$_3$ after ultrafast optical excitation. Using time- and angle-resolved photoemission spectroscopy, we observe an unusual transient modulation of the relaxation rates of excited photocarriers. A detailed analysis of the electron self-energy based on a nonequilibrium Green's function formalism reveals that the phase space of electron-electron scattering is critically modulated by the photoinduced collective CDW excitation, providing an intuitive microscopic understanding of the observed dynamics.

A defining feature of metals is that they feature electronic states around the Fermi level E_F, allowing for low-energy excitations and thus enabling efficient electronic transport. A central quantity that encodes such quasiparticle excitations is the electron self-energy $\Sigma(E, \boldsymbol{k})$, which describes all interactions with the electronic quasiparticle at energy E and momentum $\boldsymbol{k}$. In simple metals, the self-energy is dominated by electron-electron (e–e) scattering and is well-described by Fermi-liquid theory [1]. However, in more complex materials, an interplay between e–e, electron-phonon (e–ph), electron-impurity scattering, and the electronic band structure, governing the available phase space for particular quasiparticle excitations, has to be considered [2]. Thus, for most materials, a quantitative theoretical treatment proves challenging[3, 4], and a detailed understanding of the self-energy – essential for disentangling the intricate interactions in complex solids – is still missing.

A key technique to investigate quasiparticle interactions in solids directly on their intrinsic timescales is time- and angle-resolved photoemission spectroscopy (trARPES) [5], in which a femtosecond (fs) optical pump pulse generates an excited-carrier population. Probing the transient quasiparticle band structure by a time-delayed UV/XUV pulse during the subsequent recovery elucidates charge- and energy redistribution processes and allows disentangling competing contributions to the self-energy [6–13]. Additionally, optical excitation allows for transient manipulation of specific material properties with high selectivity by tailoring the excitation wavelength, polarization, pulse energy, and length. Prominent examples of this rapidly growing research field include photostabilization of superconductivity[14, 15], dynamical modification of the band structure due to the formation of photon-dressed states[16, 17], and stabilization of metastable states not accessible in thermal equilibrium[18, 19]. Intriguingly, time-domain studies offer a natural route to access the transient quasiparticle interactions during the optical control of condensed matter properties, providing an understanding on the microscopic level of the self-energy.

An ideal testbed to apply this approach of studying quasiparticle interactions upon optical control are charge density waves (CDWs). This ubiquitous symmetry-broken ground state is characterized by a periodic charge- and lattice superstructure that opens up an electronic energy gap at E_F. Photoexcitation allows manipulating the system's underlying potential energy surface (PES), which triggers a transient melting of the CDW state, i.e., a photoinduced insulator-to-metal transition [20]. This intriguing nonequilibrium setting raises the question of how the ultrafast redistribution of spectral weight near E_F acts on the electron self-energy and, in particular, which scattering channels are affected.

Here, we use trARPES to investigate the electron dynamics of a prototypical CDW compound of the rare-earth tritelluride family, TbTe$_3$, after ultrafast near-infrared excitation, as illustrated in Fig. 1(a). In this material class, strong photoexcitation transforms the ground-state double-well PES to a single-well shape, sketched in Fig. 1(b), which initiates a melting of the CDW, as the system relaxes towards the new minimum corresponding to the metallic phase. However, for sufficiently strong excitation, the system overshoots across the minimum to the other side of the potential, leading to a reemergence of the CDW, followed by several damped oscillation cycles between metallic and CDW order [21–23], evident from a transient modulation of the CDW energy gap [24]. Besides the collective CDW excitation, we track the photocarrier population of high-energy states and discover a concurrent oscillation of scattering rates at the exact frequency of the CDW modulation. We find that relaxation of hot photocarriers accelerates when the system is in the metallic phase and slows down when the CDW gap reopens. To understand the underlying microscopic scattering processes, we employ a time-dependent nonequilibrium Green's function formalism (td-NEGF) [25–27], which reveals that the CDW gap opening critically reduces the phase space of e–e scattering, while e–ph scattering remains unaffected in the examined energy range.

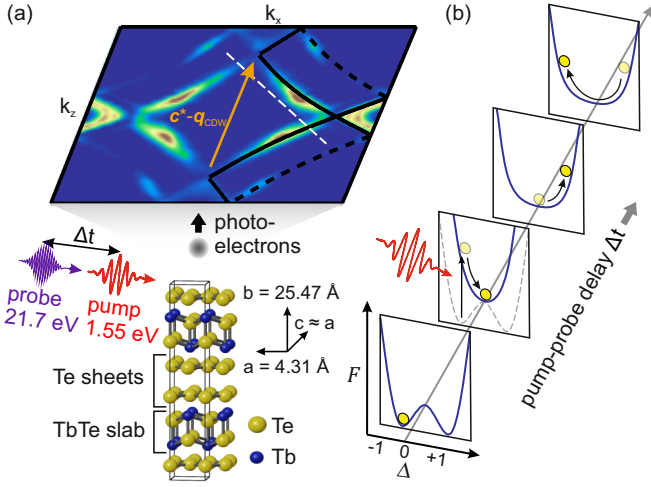We perform trARPES measurements on single crystals of

FIG. 1. Experimental scheme. (a) Top: Symmetrized FS of TbTe$_3$ ($T = 100$ K) with tight binding calculations of main (solid) and 3D-backfolded (dashed) bands. Spectral weight along the segments connected by the nesting wave vector $\mathbf{c}^*$-$\mathbf{q}_{CDW}$ is strongly reduced. The white dashed line marks the momentum cut discussed in Fig. 2. Bottom: Quasi-2D atomic structure of TbTe$_3$ consisting of TbTe slabs and Te sheets. By convention, the in-plane crystal directions are along the a and c (k$_x$ and k$_z$) axes. (b) Schematic PES as a function of pump-probe delay after photoexcitation. The yellow circle indicates the system´s order parameter, a metric for the degree of symmetry-breaking of the CDW-to-metal transition, with $|\Delta| = 0$ in the metallic and $0 < |\Delta| \leq 1$ in the CDW phase. Photoexcitation transforms the ground-state double-well potential into a high-symmetry state, launching an oscillation between metallic and CDW phase.

TbTe$_3$ as described earlier [24]. The setup includes a tabletop fs XUV source ($h\nu_{probe} = 21.7$ eV) with a synchronized optical pump laser ($h\nu_{pump} = 1.55$ eV), using a hemispherical analyzer for photoelectron detection [28]. The ultimate time and energy resolutions are ~ 35 fs and ~ 150 meV, respectively. All measurements were carried out in $p < 1 \times 10^{-10}$ mbar and at $T = 100$ K, well below the transition temperature $T_c = 336$ K of the unidirectional CDW phase of TbTe$_3$ [29]. Note that in rare-earth tritellurides strongly wave-vector dependent e–ph coupling [30], in conjunction with a moderately well-nested Fermi surface (FS) [31], leads to a unidirectional CDW in which some parts of the FS become gapped while others remain metallic [32], see Fig. 1(a).

We investigate the electron dynamics after photoexcitation in the energy-momentum cut shown in Fig. 2(a). This allows us to simultaneously track the CDW energy gap $\Delta_{CDW}(\Delta t)$ at E_F (red arrow) and the population lifetimes of several distinct high-energy states that are transiently populated upon photoexcitation (regions of interest (ROIs) 1 and 2). As Figs. 2(b-c) show, within 140 fs after optical excitation, the CDW gap is fully suppressed, indicating a transition from the CDW to the metallic phase. However, as shown in a previous work [24], due to the substantial perturbation of the PES, the system subsequently overshoots beyond the metallic phase, followed by several weakly damped oscillations between metallic and

CDW order, see the schematic Fig. 1b.

To quantify the CDW dynamics, we estimate the transient energy gap Δ_{CDW} from the energy distribution curves (EDCs) shown in Fig. 2(c), using a leading/trailing edges approach, as discussed in the supplemental material [33]. The extracted transient Δ_{CDW} shown in Fig. 2(d) features damped oscillations at a frequency far beyond the intrinsic CDW amplitude mode – a signature of the overshoot regime [24]. Concomitantly, we track the transient photoemission intensities I at ~ 1.2 eV (ROI 1 in Fig. 2(a)) and ~ 0.8 eV above E_F (ROI 2), as shown in Figs. 2(e-f). Intriguingly, the dynamics of these excited-state populations display a clear correlation with the CDW dynamics, as they feature an exponential decay, on which weak oscillations are imprinted at the frequency of the collective CDW modulation. This oscillatory component directly reflects a modulation of the relaxation rate of the transient population [34]. In contrast, most previously investigated materials exhibit constant relaxation rates. We quantify the experimental relaxation rates employing a single-exponential decay fit, whereby we use a time-dependent 1/e lifetime $\tau_{exp}(\Delta t)$ with a damped sinusoidal contribution to account for the observed modulations [35], which yields an excellent description of the experimental data. The deviation from a bare exponential decay is emphasized by the extracted lifetimes τ_{exp} shown in Figs. 2(e-f), as they feature considerable modulations that coincide with the CDW gap dynamics: Whenever the system becomes metallic ($\Delta_{CDW} \sim 0$ eV), τ_{exp} reaches its minimum; the high-energy population relaxes faster. Conversely, when the CDW gap opens, the relaxation of the high-energy population slows down, indicated by the local maxima of τ_{exp}.

To elucidate this dynamical modulation of the relaxation, a microscopic perspective onto the scattering channels is required. To this end we employ microscopic simulations based on the td-NEGF formalism. The relevant bands are captured by the tight binding (TB) model from Ref. [32]. We consider the lesser Green's function $G^<_{(m\nu),(m'\nu')}(\mathbf{k}; t, t') = i\langle \hat{c}^\dagger_{\mathbf{k}m'\nu'}(t)\hat{c}_{\mathbf{k}m\nu}(t')\rangle$, where m, m' corresponds to the $p_{x,z}$ orbitals and $\nu = -1, 0, +1$ to the nesting index with respect to the CDW wave-vector $\mathbf{q}_{CDW}$. Computing the Green's function provides a direct link to the trARPES intensity [27, 36]:

$$I(\mathbf{k}, \omega, \Delta t) \propto \text{Im} \sum_m \int dt \int dt'\, s(t)s(t') \\ \times e^{i\omega(t-t')} G^<_{(m0),(m0)}(\mathbf{k}; t, t'). \quad (1)$$

Here, ω is the binding energy and Δt denotes the pump-probe delay, which enters the shape functions $s(t)$. While the inequivalence of single-particle and population lifetimes prohibits a direct assignment of experimental relaxation rates to quasiparticle lifetimes [9–11, 37], extracting the population dynamics from the simulated spectra (1) treats experiment and theory on equal footing and naturally includes population effects and quasiparticle decay [38, 39]. A detailed analysis of the self-energy (which determines the Green's function) allows us to connect the microscopic quasiparticle picture to the observed dynamics.
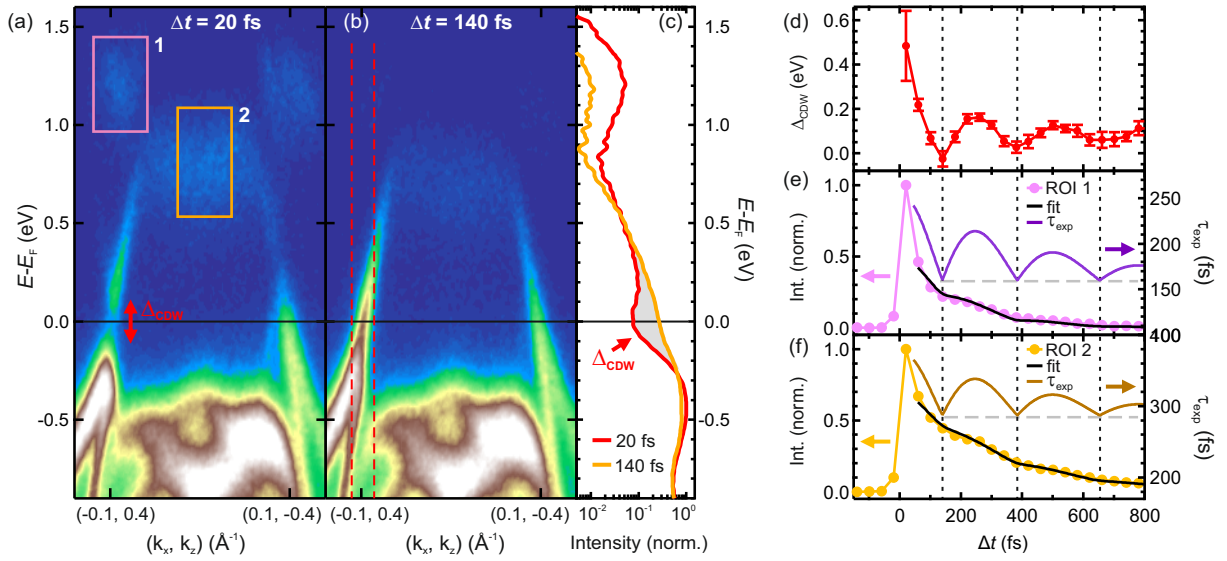
FIG. 2. Experimental band structure dynamics. (a) Energy-momentum cut along the dashed white line in Fig. 1(a) at $\Delta t = 20$ fs and (b) at $\Delta t = 140$ fs for an absorbed fluence of 0.45 mJ/cm^2. (c) EDCs of the momentum region marked by red lines in panel (b), featuring the CDW gap at E_F at $\Delta t = 20$ fs and subsequent metallization within $\Delta t = 140$ fs. (d) Extracted transient CDW energy gap with one standard deviation as uncertainty. Details of the analysis are presented in the supplemental material [33]. (e-f) Transient photoemission intensities of the ROIs indicated in panel (a) with a single-exponential decay fit (solid black line) using a time-dependent oscillatory lifetime τ_{exp} (right axis). The data point near $\Delta t = 0$ fs is excluded from the fit, as the electrons have not yet reached a thermal distribution, see supplemental material [33] for details. The dashed lines serve as guides to the eye.
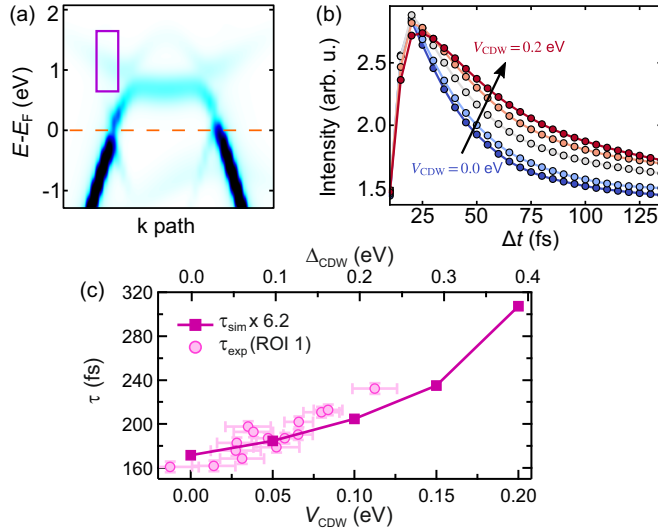

FIG. 3. td-NEGF simulations. (a) Simulated trARPES spectrum in the CDW state ($V_{CDW} = 0.2$ eV) after arrival of the pump pulse along the same momentum direction as in the experiment. (b) Intensity integrated over the ROI indicated in (a) as function of Δt for varying values of the CDW potential V_{CDW}. (c) Rescaled simulated lifetimes τ_{sim} versus V_{CDW} extracted from (b) using exponential decay fits. For direct comparison to the experiment, the transient lifetimes $\tau_{exp}(\Delta t)$ from Fig. 2(e) as function of the extracted $\Delta_{CDW}(\Delta t)$ from Fig. 2(d) are superimposed. The error bars correspond to one standard deviation of the respective fits of τ_{exp} and Δ_{CDW}.

The model parameter controlling the CDW state is the CDW

potential V_{CDW} (which corresponds to $\Delta_{CDW} \approx 2V_{CDW}$). Varying V_{CDW} leads to only minimal changes of the band structure outside of the gapped regions [40]. Hence, the observed slowdown of the relaxation dynamics must be caused by (dynamical) interaction effects. To test this hypothesis, we include e–e scattering by considering a Hubbard model with weak interaction U, which is supported by the sharpness of the bands and the rather long lifetimes observed in the experiment. We treat the e–e self-energy on the level of the second-Born approximation and employ the generalized Kadanoff-Baym ansatz (GKBA) [41]. Details are presented in the supplemental material [33].

With these ingredients, we obtain a microscopic description that captures the main features observed in the experiment. However, in contrast to the experiments, we keep the transient gap size constant during relaxation by fixing V_{CDW} to highlight the influence of the CDW state on the relaxation and to disentangle it from other effects. We simulate the GKBA time evolution upon excitation by a two-cycle pulse with $h\nu_{pump} = 1.5$ eV and calculate the trARPES signal in the full Brillouin zone (1). A typical spectrum along the same path as in Fig. 2 is shown in Fig. 3(a). We have explicitly compared the simulated and experimental spectra and optimized the field strength of the pulse to match the relative intensity shortly after the pulse in the high-energy ROI in Fig. 3(a) and close to E_F [42]. The ROI size is chosen large enough to capture the full band for any value of Δ_{CDW}, thus excluding effects attributed to shifts of spectral weight that could mask the population dynamics.

Similar to the experimental spectra we have integrated the intensity in the indicated ROI. The transient photoemission intensity as function of Δt is presented in Fig. 3(b) for different values of $V_{CDW} = 0, \ldots, 0.2$ eV (equidistant steps). For small Δt the intensity is only weakly affected by the CDW, while the long-time relaxation exhibits a pronounced dependence on V_{CDW}. In particular, the decay of intensity in the ROI is significantly faster in the metallic state ($V_{CDW} = 0$ eV). The data fit well to an exponential decay for $\Delta t > 50$ fs. Extracting the respective lifetime τ_{sim} confirms a monotonic dependence of τ_{sim} on V_{CDW}, see Fig. 3(c). For a quantitative comparison to the experimentally observed dynamical modulation of the lifetime, Fig. 3(c) also shows the experimental transient lifetime τ_{exp} of the same ROI as a function of the extracted energy gap Δ_{CDW}, which follows a similar monotonic trend. Remarkably, although the absolute simulated values are significantly shorter due to technical constraints [43], the relative change of the experimental and simulated lifetimes with Δ_{CDW} is in solid agreement.

The dependence of the lifetime τ_{sim} on V_{CDW} explains the superimposed oscillatory component of the relaxation observed in the experiment. Thermalization processes due to e–e scattering in the considered ROI are enhanced in the metallic phase, whereas the presence of the CDW gap renders scattering processes less efficient. To gain intuition on this behavior, we have analyzed the self-energy Σ^{e-e} entering the simulations in detail. In essence, the second-Born approximation captures the relaxation of an excited electron into an unoccupied lower state upon particle-hole (p–h) excitation from a lower-energy to an unoccupied higher state while obeying momentum and energy conservation. A gap near E_F suppresses the latter particle-hole transitions, hence reducing the scattering channels of highly excited electrons (Fig. 4a). Note that the CDW gap at E_F is only present at momentum points connected by $\mathbf{q}_{CDW}$; p–h excitations at E_F are still possible in other parts of the Brillouin zone. The relaxation in the upper band is thus not completely suppressed but reduced. In contrast, all p–h channels are available in the metallic phase, which increases the phase space for e–e scattering and thus enhances the relaxation rate (Fig. 4b).

This phase-space picture directly enters the Feynman diagrams for Σ^{e-e} (Fig. 4c). For an excited electron to lose the energy $\hbar\omega$ and change its momentum by $\mathbf{q}$, a corresponding p–h excitation obeying energy and momentum conservation is required. The phase-space availability of p–h processes with energy (momentum) transfer ω ($\mathbf{q}$) is captured by the p–h susceptibility $P(\mathbf{q}, \omega)$, also termed polarization in the context of many-body methods [44], illustrated in Fig. 4(c). Since small momentum transfer dominates the relaxation dynamics, we focus on the polarization $\bar{P}(\omega)$ averaged over small momenta $\mathbf{q}$. The retarded component (which is connected to the charge response, indicated by superscript R) $\bar{P}^R(\omega)$ is the relevant quantity measuring the scattering phase space and is presented in Fig. 4(d). Comparing the metallic and the CDW phase, the CDW gap opening reduces the available phase space for p–h excitations at lower energy transfer ω. Hence, corresponding
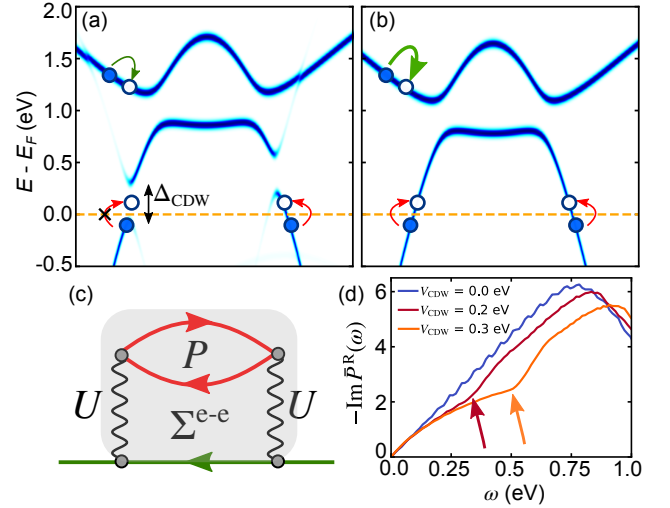

FIG. 4. Theoretical investigation of e–e scattering. Illustration of the relaxation processes by e–e scattering in (a) the CDW, and (b) in the metallic phase. The presence of a gap Δ_{CDW} in (a) suppresses p–h excitations close to the FS, limiting scattering processes in the upper band. (c) Sketch of the self-energy Σ^{e-e} diagram within the second-Born approximation. The colors are consistent with the scattering processes in (a), (b). (d) Particle-hole polarization averaged over small momentum transfer $|\mathbf{q}| < 0.05$ a.u. for different values of V_{CDW}.

relaxation processes with energy transfer ω are increasingly reduced with V_{CDW}. Consistent with experimental observations, we thus demonstrate how the photoinduced modulation of the CDW gap affects the relaxation dynamics of high-energy photocarriers.

We have also inspected e–ph scattering as a possible explanation for the observed modulation of the relaxation dynamics, calculating the e–ph self-energy Σ^{e-ph} up to second order in e–ph coupling strength assuming a Holstein model. However, there is no noticeable effect of V_{CDW} on Σ^{e-ph} in the relevant high-energy ROI [33]. The intuitive explanation is that only e–ph scattering processes close to the CDW gap are affected, whereas the presence of an energy gap near E_F does not influence e–ph scattering of high-energy electrons. Additional GKBA simulations underpin this picture [33]. Hence, we identify e–e scattering as the major relaxation mechanism in the high-energy bands, which we underpin by an intuitive picture of the CDW-induced dynamical modulation of the phase space for p–h excitations.

In conclusion, we presented a complementary experimental and theoretical study of the electron dynamics in a photoexcited charge-density-wave system, TbTe$_3$. We demonstrated how the CDW state affects the electron self-energy, resulting in a decreased relaxation rate of hot photocarriers, as the CDW gap at E_F critically restricts the phase space of electron-electron scattering. For this, we employed a combined theoretical approach, simulating population lifetimes that allow a quantitative comparison to the experimental photoelectron intensities, and scrutinizing single-particle lifetimes to gain in-

sight into the microscopic details of the interactions. While the examined setting of a collective CDW excitation is rather unique, our conclusions are independent of the details of the CDW mechanism and can be directly transferred to a broad range of materials that feature an insulator-to-metal transition. Furthermore, the array of properties that can be controlled by light is expanding rapidly. Ultrashort optical pulses allow modifying the shape and topology of the Fermi surface [45, 46], triggering collective modes that are imprinted on the electronic band structure[47, 48], and coherently modulating e–ph coupling[49]. Hence, the applied approach of tracking the fundamental interactions upon transient optical tuning may facilitate a deeper understanding of a plethora of materials.

The experimental data that support the findings of this study are publicly available [50].

Y.W.W, L.R., M.P., C.W.N. and J.M. carried out the trARPES experiments; P.W. and I.R.F. provided the samples; J.M. analyzed the data; M.Sc. performed the simulations, with guidance from M.Se.; J.M. and M.Sc. wrote the manuscript with support from L.R. and M.Se.; M.W., R.E. and L.R. provided the research infrastructure; all authors commented on the paper.

------

* Current address: Department of Physics and Fribourg Center for Nanomaterials, University of Fribourg, Chemin du Musée 3, CH-1700 Fribourg, Switzerland

† Current address: Laboratory of Ultrafast Spectroscopy, ISIC, Ecole Polytechnique Fédérale de Lausanne (EPFL), CH-1015 Lausanne, Switzerland

‡ rettig@fhi-berlin.mpg.de

[1] M. Bauer, A. Marienfeld, and M. Aeschlimann, Prog. Surf. Sci. 90, 319 (2015).

[2] E. V. Chulkov, A. G. Borisov, J. P. Gauyacq, D. Sánchez-Portal, V. M. Silkin, V. P. Zhukov, and P. M. Echenique, Chem. Rev. 106, 4160 (2006).

[3] M. Calandra and F. Mauri, Phys. Rev. B 76, 205411 (2007).

[4] P. D. C. King, S. M. Walker, A. Tamai, A. de la Torre, T. Eknapakul, P. Buaphet, S.-K. Mo, W. Meevasana, M. S. Bahramy, and F. Baumberger, Nat. Commun. 5, 3414 (2014).

[5] U. Bovensiepen and P. S. Kirchmann, Laser Photonics Rev. 6, 589 (2012).

[6] L. Perfetti, P. A. Loukakos, M. Lisowski, U. Bovensiepen, H. Eisaki, and M. Wolf, Phys. Rev. Lett. 99, 197001 (2007).

[7] P. S. Kirchmann, L. Rettig, X. Zubizarreta, V. M. Silkin, E. V. Chulkov, and U. Bovensiepen, Nat. Phys. 6, 782 (2010).

[8] S. Hellmann, T. Rohwer, M. Kalläne, K. Hanff, C. Sohrt, A. Stange, A. Carr, M. M. Murnane, H. C. Kapteyn, L. Kipp, M. Bauer, and K. Rossnagel, Nat. Commun. 3, 1069 (2012).

[9] I. Gierz, S. Link, U. Starke, and A. Cavalleri, Faraday Discuss. 171, 311 (2014).

[10] S.-L. Yang, J. A. Sobota, D. Leuenberger, Y. He, M. Hashimoto, D. H. Lu, H. Eisaki, P. S. Kirchmann, and Z.-X. Shen, Phys. Rev. Lett. 114, 247001 (2015).

[11] J. D. Rameau, S. Freutel, A. F. Kemper, M. A. Sentef, J. K. Freericks, I. Avigo, M. Ligges, L. Rettig, Y. Yoshida, H. Eisaki, J. Schneeloch, R. D. Zhong, Z. J. Xu, G. D. Gu, P. D. Johnson, and U. Bovensiepen, Nat. Commun. 7, 13761 (2016).

[12] S. Ulstrup, J. C. Johannsen, F. Cilento, J. A. Miwa, A. Crepaldi, M. Zacchigna, C. Cacho, R. Chapman, E. Springate, S. Mammadov, F. Fromm, C. Raidel, T. Seyller, F. Parmigiani, M. Grioni, P. D. C. King, and P. Hofmann, Phys. Rev. Lett. 112, 257401 (2014).

[13] E. Pomarico, M. Mitrano, H. Bromberger, M. A. Sentef, A. Al-Temimy, C. Coletti, A. Stöhr, S. Link, U. Starke, C. Cacho, R. Chapman, E. Springate, A. Cavalleri, and I. Gierz, Phys. Rev. B 95, 024304 (2017).

[14] D. Fausti, R. I. Tobey, N. Dean, S. Kaiser, A. Dienst, M. C. Hoffmann, S. Pyon, T. Takayama, H. Takagi, and A. Cavalleri, Science 331, 189 (2011).

[15] M. Mitrano, A. Cantaluppi, D. Nicoletti, S. Kaiser, A. Perucchi, S. Lupi, P. Di Pietro, D. Pontiroli, M. Riccò, S. R. Clark, D. Jaksch, and A. Cavalleri, Nature 530, 461 (2016).

[16] Y. H. Wang, H. Steinberg, P. Jarillo-Herrero, and N. Gedik, Science 342, 453 (2013).

[17] F. Mahmood, C.-K. Chan, Z. Alpichshev, D. Gardner, Y. Lee, P. A. Lee, and N. Gedik, Nat. Phys. 12, 306 (2016).

[18] L. Stojchevska, I. Vaskivskyi, T. Mertelj, P. Kusar, D. Svetin, S. Brazovskii, and D. Mihailovic, Science 344, 177 (2014).

[19] J. Zhang, X. Tan, M. Liu, S. W. Teitelbaum, K. W. Post, F. Jin, K. A. Nelson, D. N. Basov, W. Wu, and R. D. Averitt, Nat. Mater. 15, 956 (2016).

[20] F. Schmitt, P. S. Kirchmann, U. Bovensiepen, R. G. Moore, L. Rettig, M. Krenz, J.-H. Chu, N. Ru, L. Perfetti, D. H. Lu, M. Wolf, I. R. Fisher, and Z.-X. Shen, Science 321, 1649 (2008).

[21] T. Huber, S. O. Mariager, A. Ferrer, H. Schäfer, J. A. Johnson, S. Grübel, A. Lübcke, L. Huber, T. Kubacka, C. Dornes, C. Laulhe, S. Ravy, G. Ingold, P. Beaud, J. Demsar, and S. L. Johnson, Phys. Rev. Lett. 113, 026401 (2014).

[22] P. Beaud, A. Caviezel, S. O. Mariager, L. Rettig, G. Ingold, C. Dornes, S.-W. Huang, J. A. Johnson, M. Radovic, T. Huber, T. Kubacka, A. Ferrer, H. T. Lemke, M. Chollet, D. Zhu, J. M. Glownia, M. Sikorski, A. Robert, H. Wadati, M. Nakamura, M. Kawasaki, Y. Tokura, S. L. Johnson, and U. Staub, Nat. Mater. 13, 923 (2014).

[23] M. Trigo, P. Giraldo-Gallo, M. E. Kozina, T. Henighan, M. P. Jiang, H. Liu, J. N. Clark, M. Chollet, J. M. Glownia, D. Zhu, T. Katayama, D. Leuenberger, P. S. Kirchmann, I. R. Fisher, Z. X. Shen, and D. A. Reis, Phys. Rev. B 99, 104111 (2019).

[24] J. Maklar, Y. W. Windsor, C. W. Nicholson, M. Puppin, P. Walmsley, V. Esposito, M. Porer, J. Rittmann, D. Leuenberger, M. Kubli, M. Savoini, E. Abreu, S. L. Johnson, P. Beaud, G. Ingold, U. Staub, I. R. Fisher, R. Ernstorfer, M. Wolf, and L. Rettig, Nat. Commun. 12, 2499 (2021).

[25] K. Balzer and M. Bonitz, Nonequilibrium Green's Functions Approach to Inhomogeneous Systems (Springer, 2012).

[26] H. Aoki, N. Tsuji, M. Eckstein, M. Kollar, T. Oka, and

P. Werner, Rev. Mod. Phys. **86**, 779 (2014).

[27] M. Sentef, A. F. Kemper, B. Moritz, J. K. Freericks, Z.-X. Shen, and T. P. Devereaux, Phys. Rev. X **3**, 041033 (2013).

[28] M. Puppin, Y. Deng, C. W. Nicholson, J. Feldl, N. B. M. Schröter, H. Vita, P. S. Kirchmann, C. Monney, L. Rettig, M. Wolf, and R. Ernstorfer, Rev. Sci. Instrum. **90**, 023104 (2019).

[29] N. Ru, C. L. Condron, G. Y. Margulis, K. Y. Shin, J. Laverock, S. B. Dugdale, M. F. Toney, and I. R. Fisher, Phys. Rev. B **77**, 035114 (2008).

[30] M. Maschek, S. Rosenkranz, R. Heid, A. H. Said, P. Giraldo-Gallo, I. R. Fisher, and F. Weber, Phys. Rev. B **91**, 235146 (2015).

[31] J. Laverock, S. B. Dugdale, Z. Major, M. A. Alam, N. Ru, I. R. Fisher, G. Santi, and E. Bruno, Phys. Rev. B **71**, 085114 (2005).

[32] V. Brouet, W. L. Yang, X. J. Zhou, Z. Hussain, R. G. Moore, R. He, D. H. Lu, Z. X. Shen, J. Laverock, S. B. Dugdale, N. Ru, and I. R. Fisher, Phys. Rev. B **77**, 235104 (2008).

[33] Supplemental material, available online.

[34] Note that the large energy windows of the ROIs ensure that the total respective band intensities are captured during the relaxation. Thus, the transient intensity change directly reflects quasiparticle scattering.

[35] The full expression of τ_{exp} is given in the supplemental material [33].

[36] J. K. Freericks, H. R. Krishnamurthy, and T. Pruschke, Phys. Rev. Lett. **102**, 136401 (2009).

[37] V. V. Baranov and V. V. Kabanov, Phys. Rev. B **89**, 125102 (2014).

[38] A. F. Kemper, M. Sentef, B. Moritz, C. C. Kao, Z. X. Shen, J. K. Freericks, and T. P. Devereaux, Phys. Rev. B **87**, 235139 (2013).

[39] A. F. Kemper, O. Abdurazakov, and J. K. Freericks, Phys. Rev. X **8**, 041009 (2018).

[40] J. Voit, L. Perfetti, F. Zwick, H. Berger, G. Margaritondo, G. Grüner, H. Höchst, and M. Grioni, Science **290**, 501 (2000).

[41] P. Lipavský, V. Špička, and B. Velický, Phys. Rev. B **34**, 6933 (1986).

[42] The TB model does not include deeper bands from which direct transitions to ROI 2 in Fig. 2(a) occur. Therefore, we focus on the higher-energy region. The conclusions are however generic.

[43] Choosing a smaller value of U in the simulations would lead to a better quantitative agreement but requires significantly more computational resources due to the longer time scales. Additional simulations with different values of U and for an additional ROI in the supplemental material [33] corroborate the universality of the qualitative behavior.

[44] F. Aryasetiawan and O. Gunnarsson, Rep. Prog. Phys. **61**, 237 (1998).

[45] L. Rettig, R. Cortés, J.-H. Chu, I. R. Fisher, F. Schmitt, R. G. Moore, Z.-X. Shen, P. S. Kirchmann, M. Wolf, and U. Bovensiepen, Nat. Commun. **7**, 10459 (2016).

[46] S. Beaulieu, S. Dong, N. Tancogne-Dejean, M. Dendzik, T. Pincelli, J. Maklar, R. P. Xian, M. A. Sentef, M. Wolf, A. Rubio, L. Rettig, and R. Ernstorfer, Sci. Adv. **7**, eabd9275 (2021).

[47] U. De Giovannini, H. Hübener, S. A. Sato, and A. Rubio, Phys. Rev. Lett. **125**, 136401 (2020).

[48] P. Hein, S. Jauernik, H. Erk, L. Yang, Y. Qi, Y. Sun, C. Felser, and M. Bauer, Nat. Commun. **11**, 2613 (2020).

[49] Y. Zhang, X. Shi, W. You, Z. Tao, Y. Zhong, F. Cheenicode Kabeer, P. Maldonado, P. M. Oppeneer, M. Bauer, K. Rossnagel, H. Kapteyn, and M. Murnane, Proc. Natl. Acad. Sci. U.S.A. **117**, 8788 (2020).

[50] J. Maklar, Y. W. Windsor, C. Nicholson, M. Puppin, P. Walmsley, V. Esposito, M. Porer, J. Rittmann, D. Leuenberger, M. Kubli, M. Savoini, E. Abreu, S. Johnson, P. Beaud, G. Ingold, U. Staub, I. Fisher, R. Ernstorfer, M. Wolf, and L. Rettig, 10.5281/zenodo.4106272 (2020).